

# Sodium Guidestar Radiometry Results from the SOR's 50W Fasor

Jack Drummond, Steve Novotny, Craig Denman, Paul Hillman, John Telle, Gerald Moore

*Starfire Optical Range, Directed Energy Directorate, Air Force Research Laboratory  
Kirtland AFB, New Mexico 87117-5776 USA*

Mark Eickhoff

*Boeing LTS, The Boeing Company, PO Box 5670, Kirtland AFB, New Mexico 87185 USA*

Robert Fugate

*New Mexico Institute of Mining and Technology, 801 Leroy Place, Socorro, New Mexico 87801 USA*

## ABSTRACT

Having replaced our 20 W, 589 nm fasor (frequency-addition source of optical radiation) with a new fully computer automated 50 W fasor mounted to the azimuthal base of the 3.5m telescope, we have since produced a sodium laser guidestar (LGS) with a  $V_i$  magnitude of 5.1 for 30 W of fasor power in November 2005, when the annual peak in mesospheric sodium density occurs. This corresponds to a return flux at the top of the telescope of 7000 photons/s/cm<sup>2</sup> through one airmass. Late in May 2006, however, a return of only 1340 ph/s/cm<sup>2</sup> ( $V_i=6.7$ ) for 30 W of fasor power was obtained at the annual minimum in sodium column density. Earlier in the month, with 49 W of fasor power, the LGS was only as bright as  $V_i=6.3$  because of the minimum in column density. By measuring the LGS return flux in circular polarization from various altitudes and azimuths, we have detected the presence of the Earth's magnetic field, for the first time ever, as an enhancement in flux from the direction where the field lines are pointing at the SOR. We then give a formulation to predict the brightness of the LGS as a function of direction and time of year. While saturation is now being seen for linear polarization, we have seen little, if any, saturation for circular polarization at higher fasor powers, and circular produces more than twice the return of linear because of optical pumping. Finally, we have succeeded in closing the adaptive optics loop on this very bright LGS, resolving a 0.14" binary star in June 2006.

## 1. INTRODUCTION

An atomic sodium pump fasor (frequency-addition source of optical radiation) producing 20 W of power for creating a laser guidestar (LGS) for adaptive optics (AO) with a 3.5 m telescope was built at the Starfire Optical Range (SOR), a facility owned and operated by the Air Force Research Laboratory's Directed Energy Directorate on Kirtland Air Force Base near Albuquerque, New Mexico, and results have been reported previously [1-3]. That system has now been replaced by a 50 W cw fully automated fasor [4-6], and the results of sky tests in 2005 and 2006 are reported here. The fasor, itself, is continuously tunable to as fine as 60 femtometers ( $6 \times 10^{-4}$  Angstroms) across the entire sodium D2 line (FWHM  $\sim 3$  GHz) and is capable of pumping either the D2a or D2b feature with linear or circular polarization. It has far greater power than any other laser in use for astronomy and has produced the brightest guidestar to date  $V_i=5.1$ , compared to the 9th magnitude guidestar typically produced elsewhere.

## 2. RADIANCE OBSERVATIONS

### 2.1. Definition of $V_1$

In order to define the magnitude of a laser guidestar, details of the filter through which the guidestar is observed must be known and converted to a standard filter. If the area of the filter is  $A$ , found by integrating its transmission over its width, then  $A$  is also its normalized width, defined to be the width of an equivalent rectangular filter with a transmission of unity and the same area. The transmission,  $t$ , of the filter at the wavelength of the D2 sodium line, 589 nm, must also be known. For historical (and somewhat arbitrary) reasons we have defined a standard astronomical V filter to have  $A_0 = 78.5$  nm.

Observing the LGS and standard stars through the same V filter, the observed V magnitude of the LGS can be found using standard techniques with Eq 1,

$$V = a_0 + kX + v, \quad 1$$

where  $v$  is the instrumental magnitude,  $X$  is the airmass,  $k$  is the extinction coefficient, and  $a_0$  is the zero point. However, this magnitude must be standardized to the same filter across different observatories. Thus we define a  $V_1$  for the LGS which takes into account the area and transmission of the filter at  $\lambda = 589$  nm,

$$V_1 = V + 2.5 \log_{10} t - 2.5 \log_{10} (A/A_0), \quad 2$$

which can then be converted to photon flux at the top of the telescope from the LGS in photons/s/cm<sup>2</sup>,  $F$ , with

$$2.5 \log_{10} F = 14.80 + kX - V_1. \quad 3$$

### 2.2. Return Flux vs Fazor Power

Typically during sky tests, we change the power of the fazor, collect images of the LGS, and integrate them to a  $V_1$  or  $F$ , in order to plot return flux against fazor power, as in Figs 1-2. Of particular interest is the slope of these plots at the origin which should be directly related to the sodium column density. At lower power settings, as with the original 20 W system, it was sufficient to fit the data as a straight line, but at the higher power now achieved, we have begun to see some curvature to the lines which may indicate saturation. Therefore, in order to calculate the slope at the origin we have experimented with various fitting functions. In Figs 1-2 we exhibit fits with a natural log function

$$F = a \log(1 + w/w_0) \quad 4$$

which fits preliminary theoretical data quite well for linear polarization, and, in addition, in Fig 2 with a hyperbolic tangent function that may account for some additional observed variation,

$$F = a \tanh(w/w_0) + bw. \quad 5$$

In Eqs 4 and 5,  $F$  is the return flux through one airmass (overhead),  $w$  is the fazor power, and  $w_0$  is the saturation power.

In all cases, linearly polarizing the beam leads to less return and clearly shows evidence for saturation. For circular polarization, however, we have concluded that optical pumping is compensating for the expected weaker saturation (see Section 2.3), and if saturation exists it does not constitute a significant threat for lower efficiency at greater power.

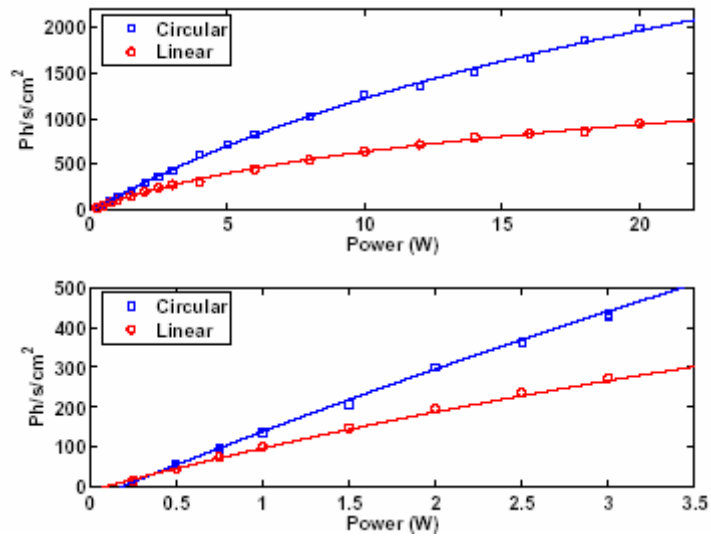


**Figure 1.** Fits of October 12, 2005, D2a line data. The lines are from a fit of the data with the Eq 4. The bottom subplot is a closeup at lower powers.

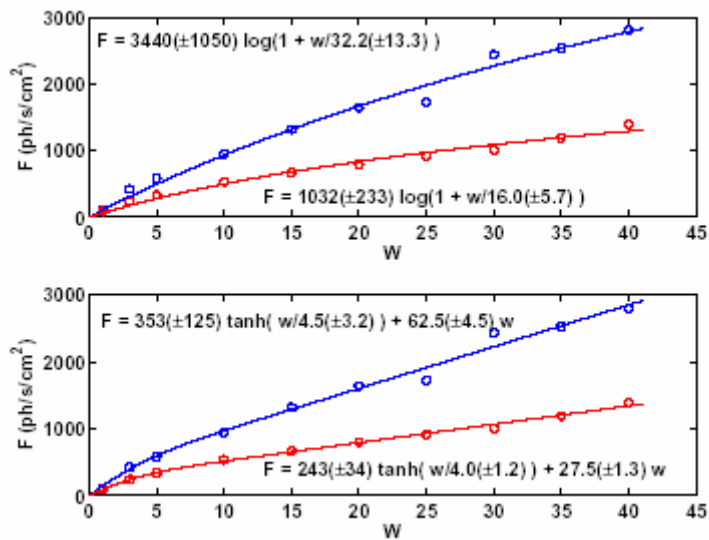


**Figure 2.** December 22, 2005 log (Eq 4) and tanh (Eq 5) fits. With more parameters, the tanh fits the data better, but it is not clear that any more than a simple log fit is justified.

### 2.3. Return Flux vs Wavelength

Another typical experiment is to change the wavelength of the faser in order to measure the brightness of the LGS as we scan the D2 line. Fig 3 shows the spectral scans from August 17, 2005, illustrating how finely we can tune the faser, and that the shape of the line, as determined from the brightness of the LGS at each wavelength, is Gaussian. Fig 4 shows spectral scans from four months in 2005. The peak of the scan with circular polarization on November 16, 2005, marks the brightest LGS achieved,  $V_1 = 5.1$  or  $F = 7000$  ph/s/cm<sup>2</sup>, even though it was produced with only 30 W of faser power. With 40 W of power in December,  $V_1 = 5.8$ , the difference being attributed to the different sodium column density on the two nights. See Section 2.4.

Notice in Fig 3 that there is a much lower return when the source is tuned to D2b (the peak at the shorter wavelength) when compared to D2a at the longer wavelength. The ratio of these two peaks should be 5.3 for sodium atoms in thermal equilibrium, whereas we have seen as much as 12.1 for circular polarization and 3.1 for linear polarization. This is evidence of strong optical pumping for circularly-polarized light and perhaps saturation for linear polarization pumping of the D2b transition. Linear polarization saturates more than circular polarization because atoms become trapped in  $F' = 1$  (the energy level associated with the D2b absorption), whereas circular polarization tends to trap atoms in a pair of states where decay into  $F' = 1$  is forbidden by selection rules, commonly referred to as optical pumping.

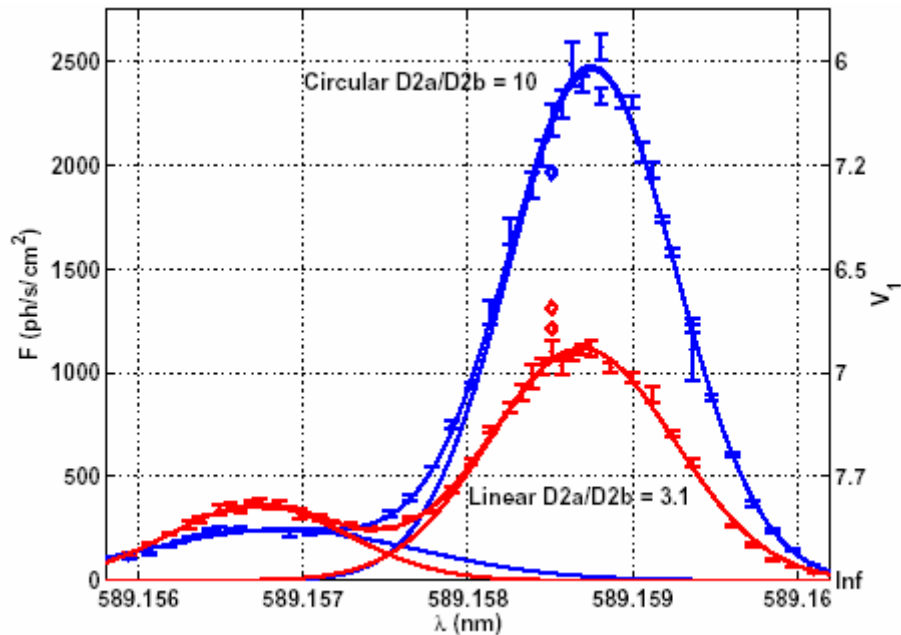


**Figure 3.** Spectral scans for circular and linear polarization, 20 W, on August 17, 2005. The lines through the data are from a simultaneous two-Gaussian fit, with the individual Gaussians for D2a and D2b also drawn.

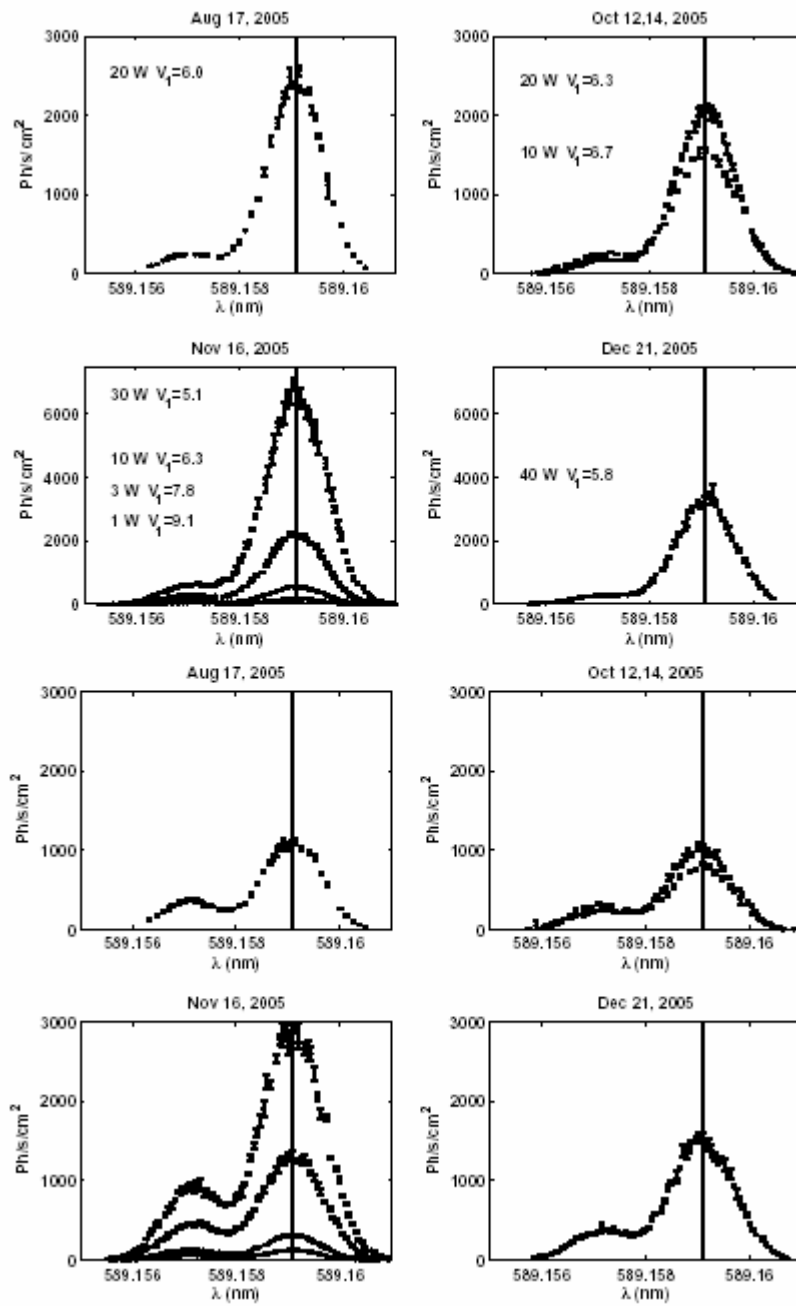


**Figure 4.** Spectral scans for circular (upper four) and linear (lower four) polarization.

### 3. VARIATION OF SODIUM COLUMN DENSITY

#### 3.1. Seasonal Variation

Determining the slope at the origin of the return flux vs laser power, using Eq 4 when possible, leads to an estimate of a quantity that should be directly related to the sodium column density. All else being equal, the greater the slope at the origin, before any saturation, the greater the sodium column density should be. Fig 5 shows this slope,  $dF/dw|_{w=0}$ , as determined over 3.5 years of sky testing.

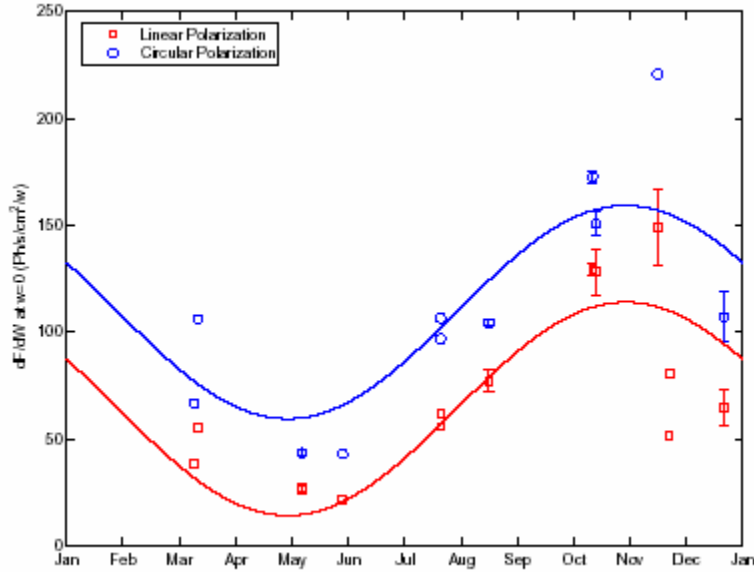


**Figure 5.** Slope,  $dF/dw$ , at laser power  $w = 0$  from our experiments over 3.5 years. The data matches the known seasonal variation of the column density. The solid lines are simultaneous fits to the annual variation with all the data, but allowing a different mean for circular and linear polarization. The largest residuals occur on November 16, during the night that the Earth goes through the Leonid meteor stream, and this may cause a spike over and beyond the annual cycle.

The fits shown in Fig 5 are from

$$S = A + B \cos((d - d_0)2\pi/365), \quad 6$$

where  $d$  is the day number since January 0,  $d_0$  is the day of maximum, and we allow a different  $A$  to be obtained for circular and linear polarization. The coefficients from the least squares fit are  $A_C = 109 \pm 9$ ,  $A_L = 64 \pm 8$ ,  $B = 50 \pm 12$ , and  $d_0 = 302 \pm 10$ . This fit for annual variation shows that the minimum occurs on April 30 and the maximum on October 30, both with an uncertainty of  $\pm 10$  days. The mean return for circular polarization is around 100 ph/s/cm<sup>2</sup>/W. The  $A_C/A_L = 1.7$  ratio indicates that circular polarization produces a 70% greater return than linear polarization, and the  $B$  to  $A$  ratio (the variation amplitude to the mean) indicates that for circular polarization the rate of return can be expected to vary by  $\pm 46\%$ , or by  $\pm 78\%$  for linear polarization.

### 3.2. Magnetic Field Detected in LGS Return

In May 2006 we measured the return flux from various elevations and azimuths, and fit the data in spherical coordinates. Combining data from May 8 and 30, 2006, the least squares fit to the return flux, uncorrected for distance or extinction, yielded Eq 7 for predicting the normalized observed brightness of the sodium LGS as a function of elevation ( $e$ ) and azimuth ( $az$ )

$$F = 0.0522 - 0.2709 \cos(e) \cos(az) - 0.1526 \cos(e) \sin(az) + 0.9478 \sin(e) , \quad 7$$

where  $F$  is the return flux in arbitrary units, normalized to one at the zenith. Since  $\cos(e) = 0$  at the zenith, the second and third terms vanish, and since  $\sin(e) = 1$  here,  $F$  is one, the sum of the first and fourth terms. Multiplying Eq 7 by either the predicted or measured brightness of the LGS at the zenith yields the actual distribution.

Figure 6 shows the results of the fit to the May 8 and 30 data, where the data from May 8 is normalized to the data at the zenith from May 30, which was the weakest return in our history. Notice that there is still an excess over the fit to the south and southwest which is interpreted as due to the Earth's magnetic field. Figure 7 shows the surface and contour plots derived from the fit. In the contour plot, the direction of the magnetic field lines at  $az = 190$  and  $e = +62$  is indicated by the X near the center of the contours at  $az = 209$ ,  $e = +72$ . Thus we conclude that the observed distribution is impacted by the Earth's magnetic field.

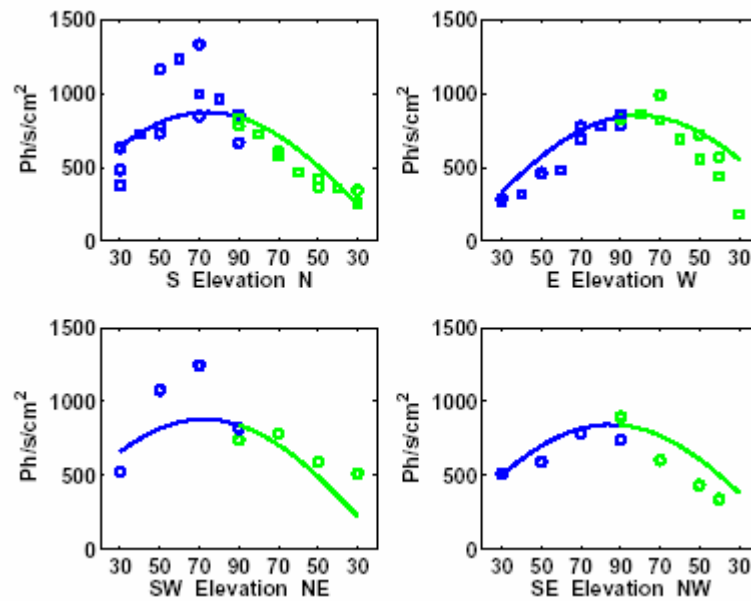


**Figure 6.** Laser return ( $\text{ph/s/cm}^2$ ) at the top of the telescope as a function of elevation for 30 W, circular polarization, normalized to May 30, 2006. Data from May 8 are indicated by squares and from May 30 by circles. The lines are the predictions from the fit (Eq 7).

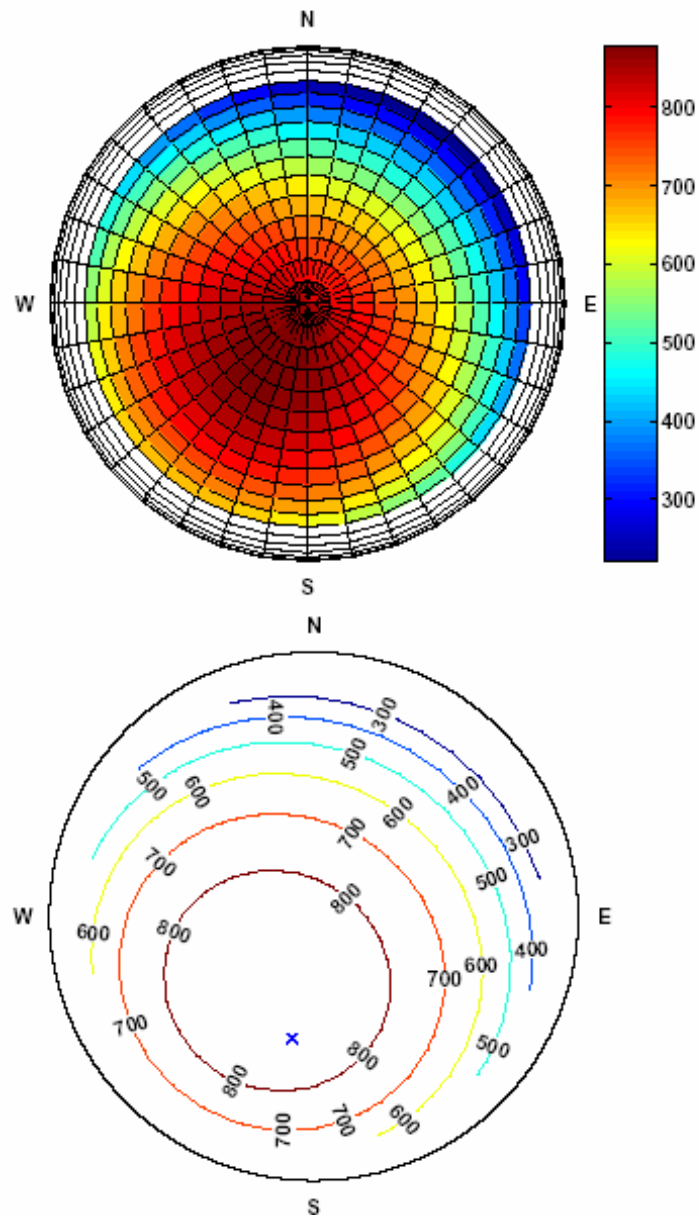


**Figure 7.** Surface and contour plots of the spherical coordinate fit to circular polarization data. The known direction where the magnetic field is aligned with the laser's pointing is marked by an x in the contour plot at  $az=190$ ,  $el=+62$ .



### 3.3. Combining Annual and Directional Models

Multiplying Eqs 6 and 7 gives a formula for predicting the return,  $F_C$ , for circular polarization as function of  $az$ ,  $el$ , faser power ( $W$ ), and day of the year.

$$F_C = FS_C W. \quad 8$$

Simply multiplying the slope  $S_C = dF/dw$  from Eq 6 or Fig 5 by the faser power to give a predicted return at the zenith may result in slightly overestimating the return if saturation occurs. However, what saturation we have encountered for circular polarization has never been significant, and a simple linear relation between faser power and return has been repeatedly justified. The uncertainties of the return flux can be gleaned from Fig 6, which shows the deviations around the fits or mean values. In particular, note the magnetic field enhancement over and beyond the fit to the south and southwest. There is an additional hourly variation of the flux associated with the variation of the column density that we have not investigated. From the unpublished work of Chet Gardner and colleagues, this hourly variation is on the order of 30% of the mean. Roughly three hours before midnight the sodium column density reaches its minimum at 0.7 times the mean for the night, and five hours after midnight it reaches its maximum at 1.3 times the mean. In other words, the mean density can vary by a factor of 1.9 during a single night. This would induce a similar variation in the return flux, and should be compared to a variation over the year of 2.75, and a variation around the sky of 4 between [209;+72] and [29;+30].

## 4. RESOLVING BINARIES WITH THE LGS

While the emphasis here has been on the radiometry of the LGS, we end with our most significant accomplishment to date, closing the AO high order loop with the LGS and imaging binaries that are too faint and close for our natural guidestar mode. While closing the high order loop with the sodium wave front sensor at 500 Hz and tracking with a pyramid tracker, AO images of six binaries were recorded at 0.85  $\mu\text{m}$  on June 6, 2006, and shown in Fig 8. The six open loop images (while tracking) are shown in Fig 9. The Strehls for the closed loop images are only 0.03, but this is as predicted for our first draft system, and is sufficient to obtain astrophysically significant quantities such as magnitude differences, separations, and orientations of faint binaries.

## 5. REFERENCES

1. Drummond, J., J. Telle, C. Denman, Paul Hillman, and A. Tuffli, Photometry of a Sodium Laser Guidestar from the Starfire Optical Range, *PASP*, **116**, 278-289, 2004.
2. Drummond, J., J. Telle, C. Denman, P. Hillman, J. Spinhirne, and J. Christou, Photometry of a Sodium Laser Guidestar from the Starfire Optical Range. II. Compensating the Pump Beam, *PASP* **116**, 952-964, 2004.
3. Denman, C., P. Hillman, G. Moore, J. Telle, J. Drummond, A. Tuffli, 20 W CW 589 nm sodium beacon excitation source for adaptive optical telescope applications, *Opt. Mat.* **26**, 507-513, 2004.
4. Fugate, R., C. Denman, P. Hillman, G. Moore, J. Telle, I. De La Rue, J. Drummond, J. Spinhirne, Progress toward a 50-watt facility-class sodium guidestar pump laser, *SPIE* **5490**, 1010-1020, 2004.
5. Telle, J., J. Drummond, C. Denman, P. Hillman, G. Moore, S. Novotny, and R. Fugate, Studies of a mesospheric sodium guidestar pumped by continuous-wave sum-frequency mixing of two Nd:YAG laser lines in lithium triborate, *SPIE* **6215**, 2006.
6. Denman, C., J. Drummond, M. Eickhoff, R. Fugate, P. Hillman, S. Novotny, and J. Telle, Characteristics of sodium guidestars created by the 50-watt FASOR and first closed-loop AO results at the Starfire Optical Range, *SPIE* **6272**, 62721L-12, 2006.

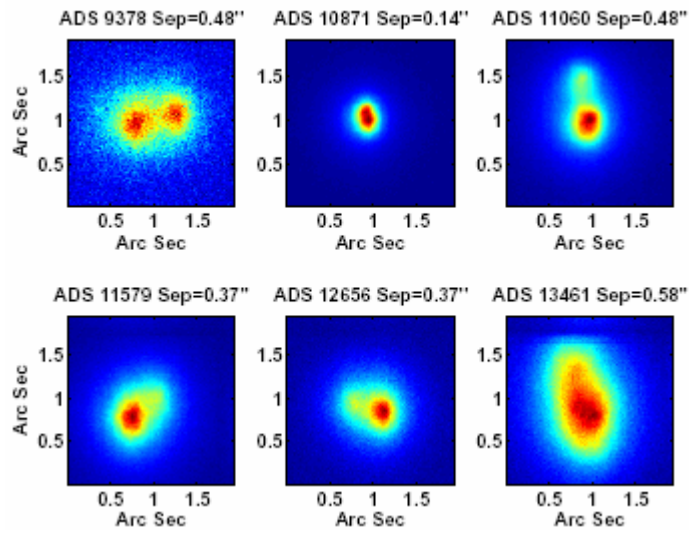


**Figure 8.** AO images of six binaries recorded at a wavelength of  $0.85\mu\text{m}$ . The high order loop was closed with the sodium wave front sensor at  $0.59\mu\text{m}$ . Each image is comprised of 10 shift-and-add one second exposures. The brightest component is  $V=7.39$  in ADS 11060 and the faintest is 9.83 in ADS 13461.

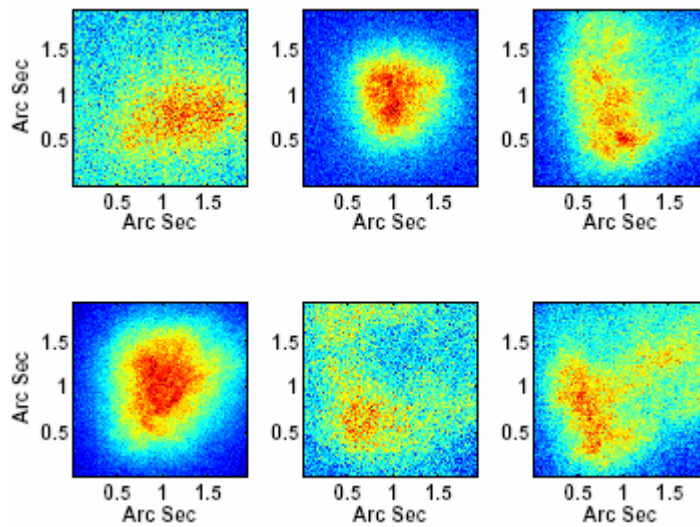


**Figure 9.** Corresponding open loop images of the six binaries in Fig 8. With the track loop closed but the sodium LGS higher order loop open, these one second images do not reveal the stars binary nature.